Phosphate-hydrolysis, antioxidant, DNA binding, and nuclease activities promoted by heteroleptic nickel(II) phenolate complexes

ARTICLE *in* MEDICINAL CHEMISTRY RESEARCH · DECEMBER 2014

Impact Factor: 1.4 · DOI: 10.1007/s00044-014-1306-4

2 AUTHORS:

Perumal Gurumoorthy

The New College

9 PUBLICATIONS **26** CITATIONS

SEE PROFILE

A. Kalilur Rahiman

The New College (Autonomous), Chennai, I…

50 PUBLICATIONS **400** CITATIONS

SEE PROFILE

Med Chem Res (2015) 24:2441–2453
DOI 10.1007/s00044-014-1306-4

MEDICINAL CHEMISTRY RESEARCH

ORIGINAL RESEARCH

Phosphate-hydrolysis, antioxidant, DNA binding, and nuclease activities promoted by heteroleptic nickel(II) phenolate complexes

Perumal Gurumoorthy · Aziz Kalilur Rahiman

Received: 13 August 2014 / Accepted: 29 November 2014 / Published online: 12 December 2014

Abstract Eight heteroleptic nickel(II) complexes of the type [NiL$^{1-4}$(co-ligand)] **1–8**, where L$^{1-4}$ = N^1,N^2-bis(5-substituted-2-hydroxybenzylidene)-1,2-ethylene/phenylene diimine and co-ligand = 2,2′-bipyridyl (bpy) or 1,10-phenanthroline (phen), have been synthesized and fully characterized by analytical and spectral methods. The six-coordinated octahedral geometry around the nickel(II) center was inferred from the electronic spectra of the complexes. Cyclic voltammetric studies of the complexes evidenced one-electron irreversible nature of reduction and oxidation process. The observed rate constant (k) values for the hydrolysis of 4-nitrophenylphosphate are in the range of 0.24–2.53 × 10^{-2} min^{-1}. The obtained room temperature magnetic moment values (2.96–3.31 BM) lies within the range observed for octahedral nickel(II) complexes. Antioxidant studies suggest the considerable radical-scavenging potency of the complexes against DPPH radical. The DNA-binding studies of complexes with calf thymus DNA revealed intercalation with minor-groove mode of binding. The nuclease activity on supercoiled pBR322 DNA revealed the involvement of hydroxyl radical and singlet-oxygen as reactive oxygen species and complexes encourage binding to minor-groove.

Keywords Heteroleptic nickel(II) complexes · Kinetic studies · Antioxidant DNA binding · Nuclease activity

Introduction

Deoxyribonucleic acid (DNA) plays a significant role in the life process and a major intracellular target molecule for most anticancer and antiviral therapies. The interaction of transition metal complexes with DNA is an important essential issue in life sciences (Zhang *et al.*, 2001; Kostova, 2005; Brabec and Nováková, 2006), and the studies of DNA-complex interaction are becoming most important to explore the possible effective chemo-agent. There is growing interest in exploring the DNA-binding mode of metal complex, aiming to a rational design and construction of new and effective DNA-targeted drug (Yola and Özaltin, 2011). Three binding modes of small molecules with double-helix DNA exist in a non-covalent way: electrostatic interaction, groove, and intercalative binding. Among them, the most effective mode of the drug targeted to DNA is intercalative binding, which is related to the anticancer activity of the molecule (Tan *et al.*, 2009). Intercalators as with groove binders can also be used for clinical treatment of cancer, fungal, and bacterial infections (Bischoff and Hoffmann, 2002). Generally, antioxidant active molecules have been found to possess anticancer, anticardiovascular, anti-inflammatory, and many other biological activities (Sankaran *et al.*, 2010). In addition, the development of artificial nucleases is also essential for the effective drug design (Jin and Cowan, 2005).

Transition metal ions are essential for the normal functioning of living organisms. The biologically accessible redox potentials and high nucleobase affinity are potential reagents for cleavage of DNA both hydrolytically

Electronic supplementary material The online version of this article (doi:10.1007/s00044-014-1306-4) contains supplementary material, which is available to authorized users.

P. Gurumoorthy · A. K. Rahiman (✉)
Post-Graduate and Research Department of Chemistry, The New College (Autonomous), Chennai 600 014, Tamil Nadu, India
e-mail: akrahmanjkr@gmail.com

and oxidatively (An *et al.*, 2006). In general, redox-active agents that damage DNA in vitro are thought to exhibit apoptotic activities in live cells by inducing oxidative stress and/or DNA damage (Valko *et al.*, 2004; Boerner and Zaleski, 2005). Thus, complexes appear to form intracellular redox-active molecules in tumors, which generate cytotoxic reactive oxygen species in vivo (Jansson *et al.*, 2010).

Nowadays, considerable attention has been diverted toward the biological investigations, such as antimicrobial, radical scavenging, DNA interaction, and anticancer activity, of transition metal complexes containing an azomethine group (–HC=N–) (Genc *et al.*, 2014; Terenzi *et al.*, 2014). Azomethine ligands form an important class of organic ligands with a wide variety of biological properties (Witkop and Ramachandran, 1964). Therefore, it is not surprising that such transition metal compounds are of great interest as potent drugs. Hetero-aromatic diimine systems like 2,2′-bipyridyl (bpy), 1,10-phenanthroline (phen) are chelating bidentate ligands for transition metal ions that have played a significant role in the development of coordination chemistry (Summers, 1978; Sammes and Yahioglu, 1994). These are rigid planar, hydrophobic, electron-deficient hetero-aromatic systems whose nitrogen atoms are appropriately placed to act cooperatively in cation binding. Heteroleptic or mixed-ligand complexes have attracted special attention due to their varied molecular geometry, DNA structural selectivity, and great DNA-binding affinity (Kurdehar *et al.*, 2011; Barone *et al.*, 2013; Ravichandran *et al.*, 2014).

Although DNA interaction with the lot number of heteroleptic complexes previously appeared in the literature, there is still scope to design and study Schiff base with metal salt as new chemical nucleases. The diversified applications of heteroleptic complexes allow the development of methods with increased selectivity and also have great importance in the field of pharmacological and environmental chemistry (Casassas *et al.*, 1990). Nickel ion is recognized as an essential trace element for bacteria, plants, animals and humans, and the bioactive mixed-ligand nickel(II) complexes that exhibit DNA binding and cleavage activity have been reported (Raman and Mahalakshmi, 2014). We have very recently reported (Gurumoorthy *et al.*, 2015) the phosphate-hydrolysis, antioxidant, DNA interaction, and cytotoxic studies of mixed-ligand copper(II) phenolate complexes. Bearing all these facts in our mind, herein we focused on the synthesis of heteroleptic nickel(II) complexes derived from salen-type ligands (N^1,N^2-bis(5-substituted-2-hydroxybenzylidene)-1,2-ethylene/phenylene diimine) and co-ligand (2,2′-bipyridyl (bpy) or 1,10-phenanthroline (phen)). The phosphate-hydrolysis, antioxidant, DNA binding, and nuclease activities of the synthesized complexes were also studied.

Experimental

Materials

Solvents used for spectroscopic studies were HPLC grade. Chemicals were commercial product and purified by standard procedure before use. The *N*,*N*′-bis(salicylaldehyde) ethylenediimine (salen type) ligands, H_2L^{1-4}, (H_2L^1–N^1,N^2-bis (5-methyl-2-hydroxybenzylidene)-1,2-ethylenediimine, H_2L^2 –N^1,N^2-bis(5-methyl-2-hydroxybenzylidene)-1,2-phenylenediimine, H_2L^3–N^1,N^2-bis(5-bromo-2-hydroxybenzylidene)-1,2-ethylenediimine, and H_2L^4–N^1,N^2-bis(5-bromo-2-hydroxybenzylidene)-1,2-phenylenediimine) were prepared by [2 + 1] Schiff base condensation reaction (Verquin *et al.*, 2004). Nickel(II) perchlorate hexahydrate was purchased from Sigma-Aldrich, USA. Tetra (*n*-butyl)ammonium perchlorate (TBAP) purchased from Fluka, Switzerland, was used as supporting electrolyte. Calf thymus (CT) and supercoiled pBR322 DNA were purchased from Bangalore Genei (India). (*Caution*! During handling of perchlorate salts, care should be taken because of explosion).

Methods

The elemental analyses were obtained from Carlo Erba model 1106 elemental analyzer. FT IR spectra were recorded on a JASCO FT/IR-4100 spectrophotometer using KBr pellets in the range of 4,000–400 cm^{-1}. Electronic spectra of complexes were recorded in HPLC grade DMF on Agilent-8453 spectrophotometer in the range of 200–1,100 nm at ambient temperature. ESI mass spectra were recorded on Q-Tof mass spectrometer. Redox properties of complexes were performed on CHI 602D (CH Instruments Co., USA) electrochemical analyzer. The measurements were carried out under N_2 atmosphere using a three-electrode cell in which a glassy carbon, saturated Ag/AgCl, and platinum wire were used as the working, reference, and auxiliary electrodes, respectively.

General procedure for synthesis of heteroleptic nickel(II) phenolate complexes

To a methanolic solution of $Ni(ClO_4)_2{\cdot}6H_2O$ (1 mmol, 0.36 g), appropriate ligands, H_2L^{1-4} (1 mmol) in methanol:acetonitrile (4:1 v/v) solution, and equimolar triethylamine was added with stirring, followed by bpy/phen (1 mmol) in methanol at room temperature. Then, the reaction was continued for 6 h at 80 °C. After cooling, the

reaction mixture was allowed to stand at room temperature for couple of days. The solid product obtained was washed several times with cold methanol, and fully dried in vacuo.

Phosphate-hydrolysis

The hydrolysis of 4-nitrophenylphosphate (4-NPP) was carried out spectrophotometrically by choosing the strongest absorbance at 420 nm, and monitoring the increase in absorbance at this wavelength as a function of regular time intervals. This was achieved by using an equal amount of complex catalyst (10^{-3} M) and tetramethylammonium hydroxide (TMAH, 0.1 mM) and 4-NPP (0.1 M) in DMF at room temperature. A plot of $\log(A_\infty/A_\infty - A_t)$ versus time was made for each complex, and the rate constant (k) was calculated.

DPPH radical-scavenging activity

Hydrogen atom donation (or) electron (or) free radical-scavenging abilities of complexes was evaluated from the bleaching of DPPH in methanolic medium. A 0.1 mM DPPH solution was used to generate the stable radical (Cuendet *et al.*, 1997; Burits and Bucar, 2000), and the absorbance was measured for this DPPH solution at 517 nm (A_{blank}). Stock solutions of the complexes were prepared in DMF, and 1 mL solution of these complexes (50–150 μM) was added to each solution of DPPH. The reaction mixtures was incubated for 45 min at room temperature (in dark), and the absorbance of these solutions (A_{sample}) was measured at 517 nm against blank. DPPH free radical-scavenging activity (or) inhibition (I %) of DPPH radicals for the various concentrations of complexes was calculated from the following equation (Turkoglu *et al.*, 2007):

$$I\% = \left(A_{blank} - A_{sample}/A_{blank}\right) \times 100.$$

The IC_{50} values were obtained by plotting I % values as a function of complex concentrations.

DNA-binding experiments

Absorption spectral titration

Application of electronic absorption spectra in DNA interaction is one of the most effective methods to examine the binding mode and strength of metal complex with DNA. A solution of CT–DNA in Tris–HCl/NaCl buffer gave a ratio of UV absorbance at 260 and 280 nm of about 1.93:1, indicating that the DNA was sufficiently free from proteins (Marmur, 1961). Stock solution of CT–DNA was freshly prepared in Tris–HCl/NaCl buffer. The DNA concentration per nucleotide was determined using the molar absorption coefficient 6,600 M^{-1} cm^{-1} at 260 nm (Reichmann *et al.*, 1954). Stock solution of the metal complexes was prepared by using 5 % DMF in Tris–HCl/NaCl buffer and diluting suitably with corresponding buffer to the required concentration for all experiments. The binding experiments were carried out by maintaining the constant complex concentration (50 μM) and varying DNA concentration (0–500 μM). Complex-DNA solutions were allowed to incubate for 30 min at room temperature before measurements were taken. While measuring absorption spectra, equal amounts of DNA were added to both complex solutions and reference solution to eliminate the absorbance of DNA itself. Absorption titration curves were constructed from the fractional change in the absorption intensity as a function of DNA concentration (Carter *et al.*, 1989). The intrinsic binding constant (K_b) can be calculated from the following expression:

$$\frac{[DNA]}{(\varepsilon_a - \varepsilon_f)} = \frac{[DNA]}{(\varepsilon_b - \varepsilon_f)} + \frac{1}{K_b(\varepsilon_b - \varepsilon_f)},$$

where [DNA] is the DNA concentration in M (per nucleotide), ε_a is the absorption coefficient observed at a given DNA concentration, ε_f is the absorption coefficient of complex in the absence of DNA, ε_b is the absorption coefficient of complex when fully bound to DNA, and K_b is the intrinsic binding constant in M^{-1}. Each set of data was fitted to the above equation, and the plot of $[DNA]/(\varepsilon_a - \varepsilon_f)$ versus [DNA] gave a slope, and the y-intercept which is equal to $1/(\varepsilon_b - \varepsilon_f)$ and $1/K_b(\varepsilon_b - \varepsilon_f)$, respectively. The intrinsic binding constant K_b was obtained from the ratio of the slope to the intercept.

Viscosity titration

Viscometric titrations were performed with an Ostwald microviscometer (2 mL capacity) immersed in a water bath maintained at 25 ± 0.3 °C. The desired concentrations of DNA (50 μM) and complexes (0–50 μM) were prepared in Tris–HCl/NaCl buffer. Mixing of the solution was achieved by purging N_2 gas through viscometer. The flow time was measured with a digital stopwatch, and the experiment was repeated in triplicate to get the concurrent values. Data were presented as $(\eta/\eta_0)^{1/3}$ versus binding ratio ($1/R$) [Complex]/[DNA] (Cohen and Eisenberg, 1969; Friedman *et al.*, 1990), where η and η_0 are the specific viscosity of DNA in the presence and absence of complex, respectively. The values of η and η_0 were calculated from the following relation (Satyanarayana *et al.*, 1992):

$$\eta = (t - t_b)/t_b,$$

where t_b is the flow time of buffer alone, and t is the observed flow time for DNA. Relative viscosities for DNA were obtained from the relation, η/η_0.

Cyclic voltammetry

Electrochemical techniques are best complementary to other related biophysical techniques that are applied to study the interaction between redox-active molecules and biomolecules (Mahadevan and Palaniandavar, 1996). The complex and DNA solutions were prepared by using DMF and Tris–HCl/NaCl buffer, respectively. The concentrations of complexes and DNA can be taken as 0.1 mM. Solutions were deaerated by purging with N_2 gas for 10 min prior to measurements.

Nuclease activity

The nuclease activity of nickel(II) complexes on plasmid DNA (pBR322 DNA) was examined by determining their ability to convert supercoiled DNA (SC, Form I) to nicked circular (NC, Form II) and linear circular (LC, Form III) forms using agarose gel electrophoresis technique. In cleavage reactions, supercoiled plasmid pBR322 DNA (33.3 μM) was treated with nickel(II) complexes in Tris–HCl/NaCl buffer. In each experiment, cleavage of plasmid DNA was monitored by treating different concentrations of complexes (0–100 μM) with H_2O_2 (0.1 mM, co-reactant), DMSO (10 mM, hydroxyl radical scavenger), sodium azide, (20 mM, singlet-oxygen quencher), SOD (15 units, superoxide radical scavenger), and distamycin (50 μM, minor-groove binder). The samples were incubated at 37 °C for 1 h. A loading buffer containing 0.25 % bromophenol blue, 0.25 % xylene cyanol, 30 % glycerol (3 μL) was added, and the electrophoresis of cleavage products was performed on 0.8 % agarose gel containing ethidium bromide (1 μg/mL). The gels were run at 50 V for 30 min in TAE buffer (40 mM Tris base, 20 mM acetic acid, 1 mM EDTA, and pH 8.3). The bands were viewed by placing the gel on UV illuminator and photographed. The DNA ligation experiments were conducted as follows: The cleavage product of SC DNA was isolated and purified by DNA gel extraction kit. After purification, the cleaved DNA (2 μL) was incubated for 12 h at 16 °C with 1.5 μL of 10X ligation buffer, 1 μL of T4 ligase (4 units), and 2.5 μL of 1 mM ATP. Afterward, the ligation products were stained with EtBr, electrophoresed, and imaged.

Results and discussion

Chemistry

The tetradentate salen-type ligands ($H_2L^{1–4}$) were derived from 5-substituted salicylaldehydes and ethylenediamine/*o*-phenylenediamine through Schiff base condensation. The chelating bidentate co-ligands 2,2′-bipyridyl and 1,10-phenanthroline were used as hetero-aromatic system. Heteroleptic nickel(II) complexes (**1–8**) were obtained from the reaction between equimolar amount of salen and co-ligands in the presence of $Ni(ClO_4)_2{\cdot}6H_2O$ (Scheme 1). These complexes are stable and do not undergo decomposition at ambient conditions, and they are soluble in Tris–HCl/NaCl buffer, DMF, and DMSO; partially soluble in CH_3CN. All the complexes are highly stable and do not melt up to 275 °C. The analytical data (Table 1) indicate that the metal to ligand and co-ligand ratio is 1:1:1 in all complexes, and it can be represented as [$NiL^{1–4}$(co-ligand)], which is consistent with the obtained spectral reports.

Spectral characterization and mode of bonding

The IR spectra of the ligands ($H_2L^{1–4}$) and their heteroleptic nickel(II) complexes (**1–8**) were recorded and their comparative study has confirmed the formation of complexes with the proposed binding mode. Tentative assignments of these bands are given in Table 2. A comparative study reveals that certain peaks are common, and therefore only important peaks, which have been either shifted or disappeared, are discussed. The tetradentate salen ligands

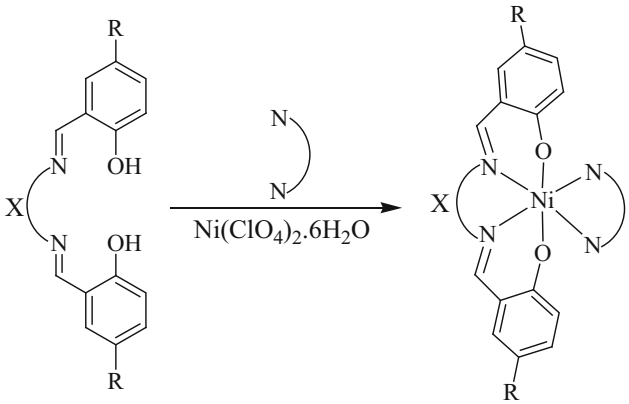

Ligands (R)	X	Complexes (N N) bpy	Complexes (N N) phen
H_2L^1 (CH_3)		1	2
H_2L^2 (CH_3)		3	4
H_2L^3 (Br)		5	6
H_2L^4 (Br)		7	8

Scheme 1 Synthesis of heteroleptic nickel(II) complexes (**1–8**)

Table 1 Elemental analyses, physico-chemical and conductivity data of the complexes (**1**–**8**)

Complex	FW (g/mol)	Yield (%)	Color	Anal. Calc. (found) (%)			Conductance (Λ_M, Ω^{-1} cm^2 mol^{-1})	μ_{eff} (BM)
				C	H	N		
[NiL^1(bpy)], **1** $C_{28}H_{26}N_4O_2Ni$	509.22	77	Light brown	66.04 (66.01)	5.15 (5.21)	11.0 (11.02)	10.8	3.31
[NiL^1(phen)], **2** $C_{30}H_{26}N_4O_2Ni$	533.25	79	Light brown	67.57 (67.53)	4.91 (4.99)	10.51 (10.54)	15.7	3.08
[NiL^2(bpy)], **3** $C_{32}H_{26}N_4O_2Ni$	557.27	84	Light brown	68.97 (68.95)	4.70 (4.78)	10.05 (10.08)	13.4	3.14
[NiL^2(phen)], **4** $C_{34}H_{26}N_4O_2Ni$	581.29	84	Brown	70.25 (70.23)	4.51 (4.60)	9.64 (9.66)	16.2	3.26
[NiL^3(bpy)], **5** $C_{26}H_{20}N_4O_2Br_2Ni$	638.96	85	Yellowish brown	48.87 (48.84)	3.16 (3.24)	8.77 (8.78)	12.0	2.98
[NiL^3(phen)], **6** $C_{28}H_{20}N_4O_2Br_2Ni$	662.98	80	Yellowish brown	50.73 (50.69)	3.04 (3.11)	8.45 (8.48)	9.1	3.04
[NiL^4(bpy)], **7** $C_{30}H_{20}N_4O_2Br_2Ni$	687.01	84	Yellowish brown	52.45 (52.43)	2.93 (3.02)	8.16 (8.19)	9.8	2.96
[NiL^4(phen)], **8** $C_{32}H_{20}N_4O_2Br_2Ni$	711.03	83	Yellowish brown	54.05 (54.04)	2.84 (2.96)	7.88 (7.93)	10.4	3.02

show broad band (due to an intramolecular hydrogen bonding (O–H…N)) in the range of 3,405–3,376 cm^{-1} corresponding to ν(O–H) stretching of phenolic group and their complexes fail to exhibit, which implies the disappearance of –OH due to deprotonation followed by complexation and water molecules in the lattice. The absence of peaks corresponding to perchlorate anions ($\sim$1,100 and 625 cm^{-1}) implies the absence of both coordinated and uncoordinated perchlorate anions in complexes. The complexes exhibit sharp bands at 1,633–1,625 and 1,548–1,536 cm^{-1} attributed to the ν(C=N) vibrations of salen and co-ligands, respectively. The azomethine vibration of complexes shifted to lower frequency (11–18 cm^{-1}) as compared to those of salen ligands, indicating the involvement of imine nitrogen in coordination to the nickel(II) ion. Coordination of imine nitrogen to the metal was expected to reduce electron density in the azomethine link which lowers the ν(C=N) vibration. The free ligands exhibit band in the region 1,295–1,287 cm^{-1} due to ν(C–O), which is shifted to higher frequency (1,316–1,307 cm^{-1}) upon complexation, suggesting the coordination via phenoxide atom. Conclusive evidence on the bonding of phenolic oxygen and azomethine nitrogen of the ligand with metal ion is also shown by the observation that new bands in the spectra of all complexes appear in the low frequency regions at 537–523 and 473–457 cm^{-1} which are characteristic to the ν(Ni–O) and ν(Ni–N) vibrations, respectively, which are not observed in the spectra of free ligands.

The ^{1}H NMR spectra (Fig. S1) of heteroleptic nickel(II) complexes show the considerable changes in the chemical shift of the proton resonances when compared with the respective salen ligands. Upon complexation, the broad signal (12.97–13.11 ppm) due to the phenolic proton of salen ligands was disappeared, which supports the coordination of phenoxide atom to nickel(II) ion. The coordinated azomethine proton signal of the complexes was observed at 8.69–8.83 ppm, and these are shifted downfield with respect to the corresponding resonance in the free ligands, indicating that the Ni–N bond is retained in solution. The aromatic signals (6.63–7.61 ppm) and aliphatic protons (methyl and methylene protons; 2.41–3.38 ppm) appear in their usual positions with considerable downfield shifts when compared with the free ligands. Further, the complexes show an imine proton of the co-ligands (8.19–8.34 ppm) with slight downfield shift implying the coordination of imine nitrogen to nickel(II) ion. The NMR spectra gave additional information about the structure of the complexes, which are consistent with the other spectral properties.

The electronic absorption studies allowed an insight into the coordinating behavior of the ligands to their nickel(II) complexes at room temperature. The spectra of ligands exhibit intra-ligand (π–π^* and n–π^*) transitions in the region of 238–406 nm, and the complexes exhibit the intra-ligand and ligand to metal-charge transfer transitions in the region 248–276 and 354–375 nm, respectively. The bathochromic shift of these charge transfer transition bands in

Table 2 Infra red spectral data (cm^{-1}) of the complexes (**1–8**)

Complex	ν(C=N), Schiff base	ν(C=N), bpy/phen	ν(C=C)	ν(C–H)	ν(Ar–O)	ν(Ni–O)	ν(Ni–N)
[NiL^1(bpy)], **1**	1,627	1,546	1,468	3,022	1,307	529	473
[NiL^1(phen)], **2**	1,633	1,544	1,482	2,996	1,315	526	459
[NiL^2(bpy)], **3**	1,628	1,542	1,448	2,984	1,310	531	463
[NiL^2(phen)], **4**	1,625	1,548	1,463	3,026	1,309	537	470
[NiL^3(bpy)], **5**	1,629	1,539	1,475	3,047	1,316	529	468
[NiL^3(phen)], **6**	1,631	1,541	1,471	3,018	1,311	523	457
[NiL^4(bpy)], **7**	1,627	1,536	1,452	2,986	1,308	529	465
[NiL^4(phen)], **8**	1,629	1,540	1,469	3,008	1,314	527	471

complexes suggests the coordination of azomethine with metal center (Ainscough *et al.*, 1997). The heteroleptic nickel(II) complexes exhibit room temperature magnetic moment of 2.96–3.31 BM indicating that the Ni(II) ion is six coordinated and probably with octahedral geometry. The six-coordinated Ni(II) complexes are expected to display three spin-allowed bands corresponding to $^3A_{2g} \rightarrow {}^3T_{1g}$ (^3P), $^3A_{2g} \rightarrow {}^3T_{1g}$ (^3F), and $^3A_{2g} \rightarrow {}^3T_{2g}$ transitions (Lever, 1984). Present complexes exhibit these bands in the region 416–435, 644–660, and 963–982 nm, respectively (Fig. S2), and this augments show the geometry of the central metal(II) ion as octahedron. The ESI mass spectra of the complexes were studied in positive mode, which supports the formation of the heteroleptic nickel(II) complexes, showing *m/z* ion peak corresponding to the molecular weight of complexes (Fig. S3). The intensities of peaks are in accordance with the abundance of the ions. The information gathered from ESI mass data agrees well with the elemental analysis data.

From the above discussions, it is concluded that all the salen ligands behave as dianionic tetradentate ligand with N_2O_2 donor sites. In complexes **1–8**, four of the six coordination sites of octahedron are occupied by salen ligand through two nitrogen atoms of azomethine groups and two oxygen atoms of phenoxide ions, whereas fifth and sixth coordination positions are occupied by two nitrogen atoms of the co-ligand. On the basis of above conclusions, the optimized structure of the complex **8** is depicted in Fig. 1.

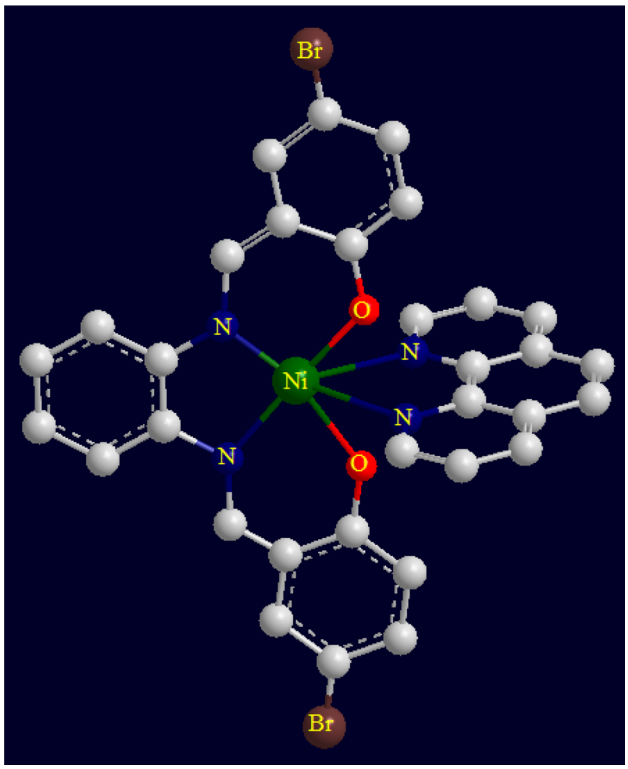

Fig. 1 The optimized structure of heteroleptic nickel(II) complex **8**

Electrochemical properties

The molar conductance (Λ_M) values of the heteroleptic nickel(II) complexes (**1–8**) are found to be 9.1–16.2 Ω^{-1} cm^2 mol^{-1} in 10^{-3} M DMF, indicating the non-electrolytic nature of the complexes (Geary, 1971).

Electrochemical properties of the complexes depend on number of factors such as chelation, axial ligation, degree, and distribution of unsaturation and substitution pattern (Benzekri *et al.*, 1991). The cyclic voltammetric data of the heteroleptic nickel(II) complexes versus Ag/AgCl electrode at 100 mV/s scan rate (ν) are summarized in Table 3. The observed irreversible reduction (Fig. S4) and oxidation waves (Fig. S5) of the nickel(II) complexes represent one-electron transfer in the region of −0.798 to −0.743 V and +0.982 to +1.053 V, respectively. The voltammetric results show that the redox peak potential (E_{pc}) varies as it can be expected from the electronic effects of the substituent at para position. The complexes of electron-withdrawing substituent (Br) at the para position to the phenoxide ion are reduced at less negative potential, which decreases the electron density around the metal ion and favors easy reduction, while the electron donating group (CH_3) has a reverse effect.

Table 3 Electronic, electrochemical, initial rate constant values for hydrolysis of 4-nitrophenylphosphate and antioxidant activity data of the complexes (**1–8**)

Complex	d–d bands λ, nm (ε, M^{-} cm^{-1})	E_{pc} (V)		K (10^{-2} min^{-1})	IC_{50} (DPPH, μM)
		Reduction	Oxidation		
1	428 (3,125), 653 (765), 971 (115)	−0.778	+0.982	0.24	121.0 ± 0.4
2	431 (2,695), 657 (715), 968 (105)	−0.781	+0.974	0.37	119.3 ± 1.1
3	425 (3,045), 644 (815), 978 (135)	−0.775	+1.009	0.46	118.0 ± 1.4
4	416 (2,975), 658 (785), 982 (095)	−0.798	+0.952	0.63	114.9 ± 0.8
5	435 (2,460), 660 (695), 977 (085)	−0.743	+1.026	0.32	131.6 ± 0.7
6	420 (3,005), 649 (825), 971 (120)	−0.762	+1.021	0.41	128.2 ± 1.3
7	430 (2,970), 655 (710), 963 (065)	−0.754	+1.053	1.08	127.4 ± 0.5
8	419 (3,055), 648 (745), 974 (070)	−0.771	+1.015	2.53	125.2 ± 0.6
Vit C	–	–	–	–	132.8 ± 1.6
BHT	–	–	–	–	86.4 ± 2.5

Kinetic studies of phosphate-hydrolysis

Hydrolysis reactions in enzyme catalysis involve metal ions that are assumed to activate a water molecule which forms hydroxyl group as a nucleophile in reaction system (Rey *et al.*, 2007). The kinetic studies of the heteroleptic nickel(II) complexes (**1–8**) on hydrolysis of 4-nitrophenylphosphate were investigated spectrophotometrically at 420 nm for 45 min, and the increase in absorption due to the formation of 4-nitrophenolate anion was observed. Plots of $\log(A_\infty/A_\infty - A_t)$ versus time for hydrolysis of 4-NPP in the presence of complexes are shown in Fig. S6, and the results are depicted in Table 3. The obtained rate constant (k) values fall in the range of 0.24–2.53 × 10^{-2} min^{-1}. The results indicate that the complexes of ligands $H_2L^{3,4}$ show higher rate constant than the corresponding complexes of ligands $H_2L^{1,2}$. The structure and electrochemical properties are important phenomena in determining the catalytic activity of complexes. The complexes containing electron-withdrawing group show higher catalytic activity than complexes containing electron-releasing group as the presence of electron-withdrawing group reduces the electron density around the metal ion and favors easy reduction (MacLachlan *et al.*, 1996).

In vitro antioxidant activity

The evaluation of DPPH radical-scavenging activity is a standard assay in antioxidant studies, and offers a rapid technique for screening the radical-scavenging property of specific compounds or extracts (Amarowicz *et al.*, 2004). In general, many bioredox processes generate free radicals, which may induce oxidative damage in various components of the body including lipids, proteins, and DNA, and have been implicated in aging and a number of life-limiting chronic diseases (cancer, hypertension, cardiac infarction, atherosclerosis, rheumatism, cataracts, etc.,) (Tsai *et al.*, 2001). Efforts to counteract the damage caused by these species are gaining acceptance as a basis for novel therapeutic approaches, and the field of preventive medicine is experiencing an upsurge of interest in useful antioxidants.

DPPH radical is a stable free radical showing a strong absorption band at 517 nm due to the presence of an odd electron. When this electron becomes paired off by accepting an electron or hydrogen radical, the absorption decreases stoichiometrically with respect to the number of electrons or hydrogen atoms taken up. Hence, more rapidly the absorbance decrease, the more potent is the antioxidant activity of the complex, and the activity was determined in terms of IC_{50} values. The scavenging activity of the complexes was also compared with those of the well-known natural and synthetic antioxidants, vitamin C (Ascorbic acid), and BHT (Butylated toluene), respectively. In vitro antioxidant results (Table 3) strongly support the better scavenging activity of the complexes against DPPH radical. All the complexes showing better scavenging activity could be due to coordination of metal after complexation of the system, increasing its capacity to stabilize the unpaired electron and thereby, and to arrest the free radicals. The antioxidant potency (IC_{50}) follows the order BHT > **4** > **3** ≥ **2** > **1** > **8** > **7** ≥ **6** > **5** > Vitamin C. The effect of scavenging property (Fig. 2) varies by changing the substituent in ligand. Electron-releasing substituent present in the ligand shows higher activity than the electron-withdrawing group. Although the mechanism of radical-scavenging activity of complexes under study remains unclear, these experimental results are helpful in designing more potent scavengers. The antioxidant activity of these nickel(II) complexes is comparable to the previously reported similar mixed-ligand copper(II) phenolate complexes (Gurumoorthy *et al.*, 2015). In view of the observed

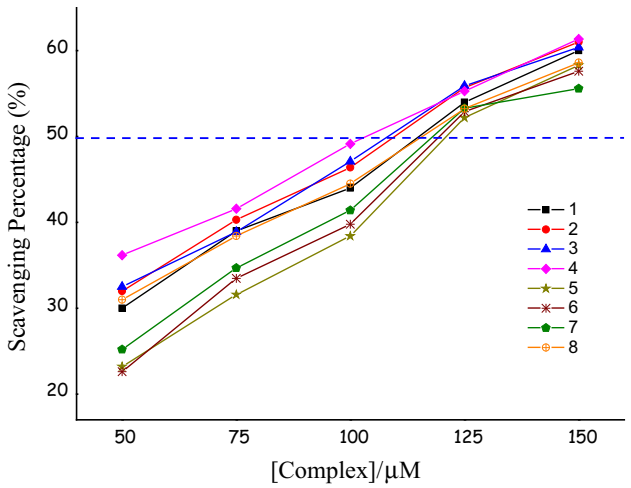

Fig. 2 DPPH radical inhibition effects of heteroleptic nickel(II) complexes (**1**–**8**)

antioxidant results, the Ni(II) complexes can be considered as potential drugs to eliminate the DPPH radical.

Stability test of complexes

Tris–HCl/NaCl buffer was used as medium for DNA binding and nuclease activity, so it was necessary to examine the stability of heteroleptic nickel(II) complexes in this buffer. A negligible absorbance and current change were observed after 48 h in electronic spectra and cyclic voltammetry, respectively. Negligible absorbance/current change without any considerable shift in wavelength/potential predicted the stability of complexes in Tris–HCl/NaCl buffer.

DNA-binding studies

Absorption spectral titration

Electronic spectroscopy is one of the most convenient tools to examine the binding mode and strength of complexes with CT–DNA. The drug-DNA interaction can be carried out by monitoring the changes in the absorption properties of the drug or DNA molecules. The interaction between the complexes and DNA is expected to perturb the ligand-centered transitions of complex. Usually, the molecules bind with DNA through both covalent and/or non-covalent interactions, such as intercalation, electrostatic, and groove (major/minor) binding. Intercalative drugs bind with DNA following the hypochromism and red shift due to the strong stacking interaction between the aromatic chromophore of ligand and DNA base pairs, with the extent of hypochromism commonly consistent with the strength of intercalative binding (Chao *et al.*, 2002).

DNA-binding experiments of the heteroleptic nickel(II) complexes were performed in Tris–HCl/NaCl buffer by adding increments of DNA stock solution to a fixed complex concentration (Fig. 3). The increase in concentration of CT–DNA results in the minor bathochromic shift (1–2 nm) with considerable hypochromicity (19–31 %) which implies that all the complexes bind with DNA via intercalation. Strength of intercalative binding of molecules to DNA is known to cause hypochromism with much larger bathochromic shift of the spectral bands (Nair *et al.*, 1998). Hence, from the observed hypochromism and least bathochromic shift, we could suggest the possibility of partial intercalation with groove binding of complexes with CT–DNA (Maity *et al.*, 2009). The intrinsic binding constant (K_b) of complexes was calculated and found in the range of 0.78 (±0.4)–1.06 (±0.3) × 10^5 M^{-1} (Table 4). The binding strength of complexes is comparable with the binding strength of reported heteroleptic nickel(II) (Raman and Mahalakshmi, 2014) and copper(II) (Gurumoorthy *et al.*, 2015) complexes, but lower than that of classical intercalators (EtBr and $[Ru(phen)_2(dppz)]^{2+}$), in which the binding constants have been found to be in the order of 10^6–10^7 M^{-1} (Cory *et al.*, 1985).

The methyl-substituted complexes show higher binding propensity due to hydrophobic interaction of methyl group with the hydrophobic DNA surface that leads to the enhancement of DNA-binding affinity. Further, the complexes containing phen as co-ligand exhibit higher DNA-binding propensity due to the presence of an extended aromatic ring, which might facilitate partial intercalation of the base through non-covalent π–π interaction with the DNA bases.

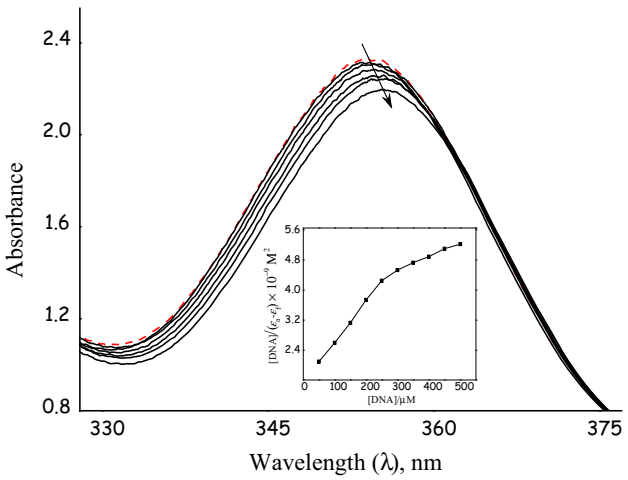

Fig. 3 Absorption spectra of complex **4** (50 μM) in Tris–HCl/NaCl buffer upon addition of CT–DNA (0–500 μM). *Arrow* shows the absorption changes upon increasing concentration of DNA. *Inset* Plot of [DNA]/(ε_a−ε_f) versus [DNA] for absorption titration of CT–DNA with complexes

Table 4 Absorption spectral data for DNA binding of the complexes (**1–8**)

Complex	λ (nm)	Change in Absorption/Wavelength	$\Delta\lambda$/nm	H (%)[a]	K_b (10^5 M^{-1})
1	357	Hypochromism/Red shift	1.5	24	0.9 ± 0.05
2	375	Hypochromism/Red shift	1.5	30	0.97 ± 0.06
3	363	Hypochromism/Red shift	2	28	0.92 ± 0.07
4	354	Hypochromism/Red shift	2	31	1.06 ± 0.03
5	371	Hypochromism/Red shift	1	19	0.78 ± 0.04
6	366	Hypochromism/Red shift	1	23	0.84 ± 0.03
7	358	Hypochromism/Red shift	1	22	0.81 ± 0.09
8	360	Hypochromism/Red shift	1.5	24	0.85 ± 0.02

[a] $H\ \% = [(A_{free}–A_{bound})/A_{free}] \times 100$. Measurements were made at $R = 10$, where R = [DNA]/[Complex]; [DNA] = 0–500 μM; [Complex] = 50 μM

Viscosity titration

Hydrodynamic methods that are sensitive to length are regarded as one of the least ambiguous and most critical methods in predicting the binding mode of complexes with DNA in solution in the absence of crystallographic data (Kamatchi *et al.*, 2013). In order to clarify the binding mode and strength of complexes (**1–8**) with CT–DNA, the DNA viscosity variance at 25 °C was achieved by varying the concentration of added complexes. Intercalating agents are expected to elongate the double helix to accommodate the ligands in between the base leading to an increase in the viscosity of DNA (Leng *et al.*, 2003). In contrast, partial intercalation or non-classic intercalation of complex would bend or kink the DNA helix, shortening the effective length of DNA, and reducing DNA viscosity accordingly, while the electrostatic and groove binding cause less pronounced (positive or negative) or no change in DNA solution viscosity (Wang *et al.*, 2007). As a validation of the above verdict, viscosity measurements of complexes were carried out and the effects of complexes on the viscosity of DNA are shown in Fig. S7.

The plots of relative specific viscosity $(\eta/\eta_0)^{1/3}$, (where η and η_0 are the specific viscosity of DNA in the presence and absence of complex, respectively) versus $1/R$ ([Complex]/[DNA] = 0.1–1), show only a minor change indicating groove binding along with partial intercalation for complexes. The obtained results are very similar to the behavior of well-known classical minor-groove DNA binder distamycin. The increase in viscosity of DNA by complex **4** is the highest among all complexes but lower than distamycin. The complex **4** increases the hydrodynamic length of DNA as a consequence of the untwisting of base pairs, and helical backbone of DNA is needed to accommodate the intercalators (Chen *et al.*, 2002). It is obvious that the hydrophobic interaction of methyl group with the interior of DNA grooves is also effective in increasing the length of DNA biopolymer. The viscosity enhancement for complexes containing phen co-ligand, which is higher than the corresponding complexes containing bpy co-ligand, is traced to the presence of central planar and extended aromatic ring in the former. Thus, all these observations suggest that it is the aromatic rings, which are involved in partial intercalative mode of binding. The observed viscosity results are consistent with our foregoing hypothesis.

Cyclic voltammetry

Electrochemical techniques are extremely useful in probing the binding mode and nature of the complexes with DNA, and cyclic voltammetry provides additional information for the interaction of the reduced and/or oxidized form of metal with DNA. Cyclic voltammograms of the heteroleptic complexes (**1–8**) in the absence and presence of CT–DNA are shown in Fig. 4. Generally, the positive and

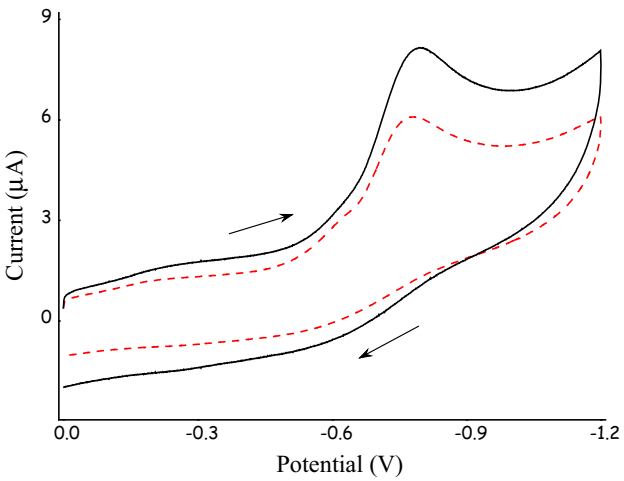

Fig. 4 Cyclic voltammograms of complex **4** in the absence (*solid line*) and presence (*dotted line*) of CT–DNA. [Complex] = [DNA] = 100 μM, scan rate was 100 mV/s

negative shift in potential attributed to intercalation and electrostatic interaction, respectively (Carter and Bard, 1987; Carter *et al.*, 1989). The incremental addition of DNA to the complexes causes a decrease in cathodic peak current with no new redox peaks. The decrease in current intensity may be due to the diffusion of an equilibrium mixture of free and DNA-bound complex to the electrode surface, which suggests the existence of an interaction between each complex and DNA (Zampakou *et al.*, 2013). All the complexes exhibit same electrochemical behavior upon addition of DNA, and for increasing amounts of DNA, the potentials (E_{pc}) exhibit a positive shift ($\Delta E_p = 0.010$–0.024 V). This results show that complexes stabilizes the duplex (GC pairs) by intercalating way. Upon addition of DNA, the decrease in peak current and negative shift is higher for complex **4** than for other complexes, which suggest the greater binding affinity, and it follows the order **4** > **2** > **3** > **1** > **8** > **6** > **7** > **5**. The electrochemical studies corroborated well with the titration studies and thereby authenticate the strong interaction of CT–DNA with complexes.

Nuclease activity

Hydrolytic method of cleavage

The DNA cleavage ability of metal–ligand systems can be achieved by targeting the phospho-diester linkage, deoxyribose sugar, or nucleobase moieties of DNA. The cleavage efficacy of heteroleptic complexes (**1**–**8**) was observed in the absence of co-reagents (Fig. 5) and the increasing intensity of NC form was found with the increase in complex concentration (Lanes, 2–7). At 100 μM concentration, all the complexes cause complete cleavage into NC form, and the gel pattern indicates the single-strand DNA cleavage. As anticipated, no significant cleavage was observed for complex-free DNA (Lane 1).

The complex-DNA interaction was concluded as follows from the gel pattern results and literature (Reddy *et al.*, 2004; Desbouis *et al.*, 2012): The molecule may bind with the phospho-diester bond of DNA through the coordinate linkage and/or electrostatic interaction, and the metal center activates the central phosphorus atom of DNA, resulting in the formation of phosphorus intermediate. Then, the activated phosphorus atom is attacked nucleophilically by the metal ion due to their Lewis acidity via charge neutralization, and finally one of the phosphodiester bond of the nucleic acid is cleaved. The degree of interaction of the synthesized complexes with DNA follows the same order of DNA-binding ability. The difference in cleavage ability of complexes may be due to the influence of substituents and co-ligands present in the complexes. Therefore, similar to spectroscopic experiments on DNA binding, complex **4** proves stronger DNA cleavage than the other complexes, and the cleavage of DNA by complexes is dependent on its concentration. Thus, complex **4** with more aromatic moiety exhibits the strongest DNA binding and cleavage activity. The hydrolytic nature of the scission process was determined by using T4 ligase enzymatic assay (Fig. 5). The obtained cleavage product (NC DNA) was reacted with T4 ligase enzyme, and we have observed (Lane 8) the conversion of 65 % NC DNA to its original SC form (Sreedhara and Cowan, 1998). It is well known that in DNA hydrolytic cleavage, 3′–OH and 5′–OPO_3 (5′–OH and 3′–OPO_3) fragments remain intact and that these cleaved fragments can be enzymatically ligated (Liu *et al.*, 2002).

Investigation of reactive oxygen species (ROS)

To ascertain the increased degradation of DNA in the presence of any adventitious co-reagents, cleavage reactions were also performed by using H_2O_2, in which all complexes (25 μM) exhibit pronounced cleavage activity (Fig. 6). In the presence of a co-reagent, it is believed to produce different oxygen intermediates (ROS) depending on the specific complex and reaction conditions. A non-diffusible metal-peroxo intermediate has been invoked in

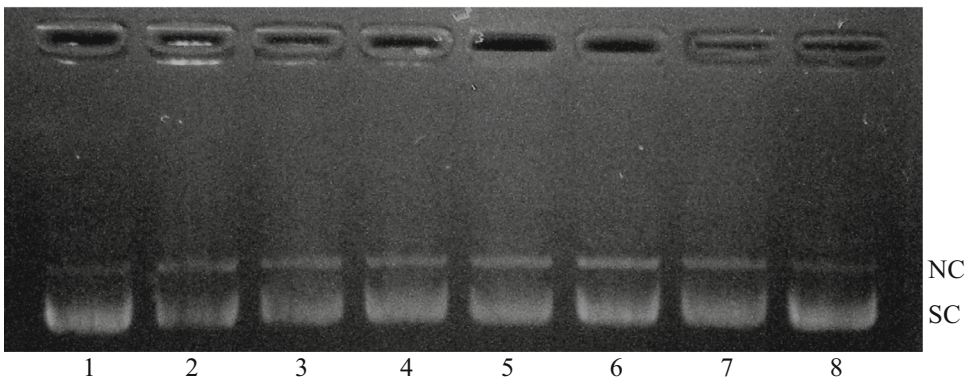

Fig. 5 Cleavage activity of complex **3** on pBR322 DNA (33.3 μM) in Tris–HCl/NaCl buffer. *Lane 1* DNA control, *Lanes 2–7* DNA + **3** (5–100 μM, respectively), *Lane 8* NC DNA (from DNA + complex) + T4 ligase enzyme (4 units)

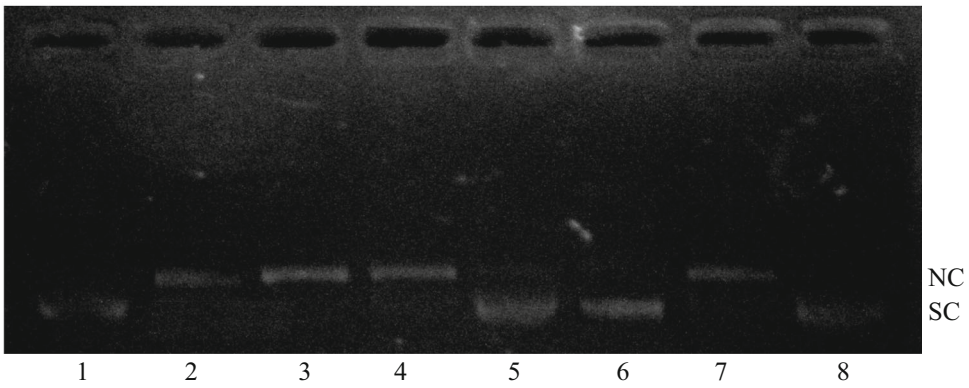

Fig. 6 Cleavage activity of complex **6** (25 μM) on pBR322 DNA (33.3 μM) in the presence of H_2O_2 (0.1 mM), DMSO (10 mM), NaN_3 (20 mM), SOD (15 units), and distamycin (50 μM) in Tris–HCl/NaCl buffer. *Lane 1* DNA control, *Lane 2* DNA + **6**, *Lane 3* DNA + H_2O_2, *Lane 4* DNA + **6** + H_2O_2, *Lane 5* DNA + **6** + H_2O_2 + DMSO, *Lane 6* DNA + **6** + H_2O_2 + NaN_3, *Lane 7* DNA + **6** + H_2O_2 + SOD, *Lane 8* DNA + **6** + H_2O_2 + distamycin

some cleavage reactions, while in others Fenton-like chemistry, which invokes release of freely diffusible hydroxyl ($OH^{\bullet}$) and/or hydroperoxyl ($HO_2^{\bullet}$) radical and/or singlet-oxygen ($^1O_2$), has been assumed. Thus, the generation of reactive hydroxyl/hydroperoxyl radical/singlet-oxygen may damage the deoxyribose ring (C3′), or alternatively a metal-peroxo species may participate directly in the oxidation of the deoxyribose ring.

To further investigate the mechanistic aspects of scission process (Scheme S1), typical scavengers such as hydroxyl radical scavenger (DMSO), singlet-oxygen quencher (NaN_3), superoxide scavenger (superoxide dismutase, SOD), and minor-groove binder (distamycin) were used in the cleavage reactions. DMSO and NaN_3 were found to inhibit some extent (Lanes 5 & 6), while the SOD showed no apparent inhibition (Lane 7), revealing that the hydroxyl radical and singlet-oxygen species are involved in the DNA scission process. The cleavage activity of complexes was inhibited in the presence of distamycin (Lane 8) suggesting DNA minor-groove binding preference for the synthesized complexes.

Conclusions

In this article, we have reported the synthesis and characterization of eight heteroleptic nickel(II) complexes of the type [NiL^{1-4}(co-ligand)], derived from salen-type ligands and co-ligands (2,2′-bipyridyl (bpy) or 1,10-phenanthroline (phen)). The analytical and spectral results suggest the octahedral geometry around the nickel(II) nuclei. All the complexes exhibit considerable catalytic and in vitro radical-scavenging activity against hydrolysis of 4-nitrophenylphosphate and DPPH radical, respectively. DNA-binding studies strongly support the partial intercalation with minor-groove binding of the synthesized complexes. The nuclease activity implies the involvement of hydroxyl radical and singlet-oxygen species in the oxidative scission process, and supports the minor-groove binding mode of complexes. The biological results indicate that complex **4** exhibits higher activities, which may be due to the presence of a hydrophobic methyl substituent and extended aromatic phen moiety. The observed results would be a great tool in the design and development of novel heteroleptic complexes as potent agent in antioxidant, DNA binding, and nuclease activity.

Acknowledgments The authors are grateful to IIT-M, Chennai, for ESI mass spectral analysis.

References

Ainscough EW, Brodie AM, Ranford JD, Waters JE, (1997) Reaction of anionic oxygen donors with the antitumour copper(II)–pyridine-2-carbaldehydethiosemicarbazone (HL) system and the crystal structure of $[\{Cu(HL)(H_2PO_4)\}_2][H_2PO_4]_2{\cdot}2H_3PO_4{\cdot}2H_2O$. J Chem Sci Dalton Trans 1251–1256. doi:10.1039/A607476F

Amarowicz R, Pegg RB, Rahimi-Moghaddam P, Barl B, Weil JA (2004) Free-radical scavenging capacity and antioxidant activity of selected plant species from the Canadian prairies. Food Chem 84:551–562

An Y, Liu SD, Deng SY, Ji LN, Mao ZW (2006) Cleavage of double-strand DNA by linear and triangular trinuclear copper complexes. J Inorg Biochem 100:1586–1593

Barone G, Terenzi A, Lauria A, Almerico AM, Leal JM, Busto N, García B (2013) DNA-binding of nickel(II), copper(II) and zinc(II) complexes: structure-affinity relationships. Coord Chem Rev 257:2848–2862

Benzekri A, Dubourdeaux P, Latour JM, Rey P, Laugier J (1991) Binuclear copper(II) complexes of a new sulphur-containing binucleating ligand: structural and physicochemical properties. J Chem Soc Dalton Trans 12:3359–3365

Bischoff G, Hoffmann S (2002) DNA-binding of drugs used in medicinal therapies. Curr Med Chem 9:321–348

Boerner LJK, Zaleski JM (2005) Metal complex-DNA interactions: from transcription inhibition to photoactivated cleavage. Curr Opin Chem Biol 9:135–144

Brabec V, Nováková O (2006) DNA binding mode of ruthenium complexes and relationship to tumor cell toxicity. Drugs Resist Updates 9:111–122

Burits M, Bucar F (2000) Antioxidant activity of *Nigella sativa* essential oil. Phytother Res 14:323–328

Carter MT, Bard AJ (1987) Voltammetric studies of the interaction of tris(1,10- phenanthroline)cobalt(III) with DNA. J Am Chem Soc 109:7528–7532

Carter MT, Rodriguez M, Bard AJ (1989) Voltammetric studies of the interaction of metal chelates with DNA. J Am Chem Soc 111:8901–8911

Casassas E, Izquierdo-Ridora A, Tauler R (1990) Electron paramagnetic resonance and visible spectroscopic studies of mixed-ligand complexes of copper(II) ion, salicylate ion, and a nitrogen base in aqueous solution. J Chem Soc Dalton Trans 8:2341–2345

Chao H, Mei WJ, Huang QW, Ji LN (2002) DNA binding studies of ruthenium(II) complexes containing asymmetric tridentate ligands. J Inorg Biochem 92:165–170

Chen HL, Liu HQ, Tzeng BC, You YS, Peng SM, Yang M, Che CM (2002) Syntheses of ruthenium(II) quinonediimine complexes of cyclam and characterization of their DNA-binding activities and cytotoxicity. Inorg Chem 41:3161–3171

Cohen G, Eisenberg H (1969) Viscosity and sedimentation study of sonicated DNA– proflavine complexes. Biopolymers 8:45–55

Cory M, Mckee DD, Kagan J, Henry DW, Miller JA (1985) Design, synthesis, and DNA binding properties of bifunctional intercalators. Comparison of polymethylene and diphenyl ether chains connecting phenanthridine. J Am Chem Soc 107:2528–2536

Cuendet M, Hostettmann K, Potterat O (1997) Iridoid glucosides with free radical scavenging properties from *Fagraea blumei*. Helv Chim Acta 80:1144–1152

Desbouis D, Troitsky IP, Belousoff MJ, Spiccia L, Graham B (2012) Copper(II), zinc(II) and nickel(II) complexes as nuclease mimetics. Coord Chem Rev 256:897–937

Friedman AE, Chambron JC, Sauvage JP, Turro NJ, Barton JK (1990) A molecular light switch for DNA: Ru(bpy)2(dppz)$^{2+}$. J Am Chem Soc 112:4960–4962

Geary WJ (1971) The use of conductivity measurements in organic solvents for the characterisation of coordination compounds. Coord Chem Rev 7:81–122

Genc ZK, Selcuk S, Sandal S, Colak N, Keser S, Sekerci M, Karatepe M (2014) Spectroscopic, antiproliferative and antiradical properties of Cu(II), Ni(II), and Zn(II) complexes with amino acid based Schiff bases. Med Chem Res 23:2476–2485

Gurumoorthy P, Mahendiran D, Prabhu D, Arulvasu C, Kalilur Rahiman A (2015) Mixed- ligand copper(II) phenolate complexes: synthesis, spectral characterization, phosphate-hydrolysis, antioxidant, DNA interaction and cytotoxic studies. J Mol Struct 1080:88–98

Jansson PJ, Sharpe PC, Bernhardt PV, Richardson DR (2010) Novel thiosemicarbazones of the ApT and DpT series and their copper complexes: identification of pronounced redox activity and characterization of their antitumor activity. J Med Chem 53:5759–5769

Jin Y, Cowan JA (2005) DNA cleavage by copper-ATCUN complexes. Factors influencing cleavage mechanism and linearization of dsDNA. J Am Chem Soc 127:8408–8415

Kamatchi TS, Chitrapriya N, Kim SK, Fronczek FR, Natarajan K (2013) Influence of carboxylic acid functionalities in ruthenium(II) polypyridyl complexes on DNA binding, cytotoxicity and antioxidant activity: synthesis, structure and in vitro anticancer activity. Eur J Med Chem 59:253–264

Kostova I (2005) Lanthanides as anticancer agents. Curr Med Chem Anti Cancer Agents 5:591–602

Kurdehar GS, Puttanagouda SM, Kulkarni NV, Budagumbi S, Revankar VK (2011) Synthesis, characterization, antibiogram and DNA binding studies of novel Co(II), Ni(II), Cu(II), and Zn(II) complexes of Schiff base ligands with quinoline core. Med Chem Res 20:421–429

Leng F, Chairs JB, Waring MJ (2003) Energetics of echinomycin binding to DNA. Nucleic Acids Res 31:6191–6197

Lever ABP (1984) Inorganic electronic spectroscopy. Elsevier, Amsterdam

Liu C, Yu S, Li D, Liao Z, Sun X, Xu H (2002) DNA hydrolytic cleavage by the diiron(III) complex Fe_2(DTPB)(μ-O)(μ-Ac)Cl(BF_4)$_2$: comparison with other binuclear transition metal complexes. Inorg Chem 41:913–922

MacLachlan MJ, Park MK, Thompson LK (1996) Coordination compounds of Schiff-base ligands derived from diaminomaleonitrile (DMN): mononuclear, dinuclear and macrocyclic derivatives. Inorg Chem 35:5492–5499

Mahadevan S, Palaniandavar M (1996) Chiral discrimination in the binding of tris(phenanthroline)ruthenium(II) to calf thymus DNA: an electrochemical study. Bioconjugate Chem 7:138–143

Maity B, Roy M, Saha S, Chakravarty AR (2009) Photoinduced DNA and protein cleavage activity of ferrocene-conjugated ternary copper(II) complexes. Organometallics 28:1495–1505

Marmur J (1961) A procedure for the isolation of deoxyribonucleic acid from micro-organisms. J Mol Biol 3:208–218

Nair RB, Tang ES, Kirkland SL, Murphy CJ (1998) Synthesis and DNA-binding properties of [Ru(NH3)4d ppz]2+. Inorg Chem 37:139–141

Raman N, Mahalakshmi R (2014) Bio active mixed ligand complexes of Cu(II), Ni(II) and Zn(II): synthesis, spectral, XRD, DNA binding and cleavage properties. Inorg Chem Commun 40:157–163

Ravichandran J, Gurumoorthy P, Imran Musthafa MA, Kalilur Rahiman A (2014) Antioxidant, DNA binding and nuclease activities of heteroleptic copper(II) complexes derived from 2-((2-(piperazin-1-yl)ethylimino)methyl)-4-substituted phenols and diimines. Spectrochim Acta A 133:785–793

Reddy PAN, Nethaji M, Chakravarty AR (2004) Hydrolytic cleavage of DNA by ternary amino acid Schiff base copper(II) complexes having planar heterocyclic ligands. Eur J Inorg Chem 7:1440–1446

Reichmann R, Rice SA, Thomas CA, Doty P (1954) A further examination of the molecular weight and size of desoxypentose nucleic acid. J Am Chem Soc 76:3047–3053

Rey NA, Neves A, Bortoluzzi AJ, Pich CT, Terenzi H (2007) Catalytic promiscuity in biomimetic systems: catecholase-like activity, phosphatase-like activity, and hydrolytic DNA cleavage promoted by a new dicopper(II) hydroxo-bridged complex. Inorg Chem 46:348–350

Sammes PG, Yahioglu G (1994) 1,10-Phenanthroline: a versatile ligand. Chem Soc Rev 23:327–334

Sankaran M, Kumarasamy C, Chokkalingam U, Mohan PS (2010) Synthesis, antioxidant and toxicological study of novel pyrimido quinoline derivatives from 4-hydroxy-3-acylquinolin-2-one. Bioorg Med Chem Lett 20:7147–7151

Satyanarayana S, Dabrowiak JC, Chaires JB (1992) Neither.DELTA.-nor.LAMBDA.- tris(phenanthroline)ruthenium(II) binds to DNA by classical intercalation. Biochemistry 31:9319–9324

Sreedhara A, Cowan JD (1998) Efficient catalytic cleavage of DNA mediated by metalloaminoglycosides. Chem Commun 16:1737–1738

Summers LA (1978) The phenanthrolines. Adv Heterocycl Chem 22:1–69

Tan J, Wang B, Zhu L (2009) DNA binding, cytotoxicity, apoptotic inducing activity, and molecular modeling study of quercetin zinc(II) complex. Bioorg Med Chem 17:614–620

Terenzi A, Bonsignore R, Spinello A, Gentile C, Martorana A, Ducani C, Högberg B, Almerico AM, Lauria A, Barone G (2014) Selective G-quadruplex stabilizers: Schiff-base metal complexes with anticancer activity. RSC Adv 4:33245–33256

Tsai K, Hsu TG, Hsu KM, Cheng H, Liu TY, Hsu CF, Kong CW (2001) Oxidative DNA damage in human peripheral leukocytes induced by massive aerobic exercise. Free Radical Biol Med 31:1465–1472

Turkoglu A, Duru ME, Mercan N, Kivrak I, Gezer K (2007) Antioxidant and antimicrobial activities of Laetiporus sulphureus (Bull.) Murrill. Food Chem 101:267–273

Valko M, Izakovic M, Mazur M, Rhodes CJ, Telser J (2004) Role of oxygen radicals in DNA damage and cancer incidence. Mol Cell Biochem 266:37–56

Verquin G, Fontaine G, Bria M, Zhilinskaya E, Abi-Aad E, Aboukaïs A, Baldeyrou B, Bailly C, Bernier JL (2004) DNA modification by oxovanadium(IV) complexes of salen derivatives. J Biol Inorg Chem 9:345–353

Wang BD, Yang ZY, Crewdson P, Wang DQ (2007) Synthesis, crystal structure and DNA-binding studies of the Ln(III) complex with 6-hydroxychromone-3-carbaldehyde benzoyl hydrazone. J Inorg Biochem 101:1492–1504

Witkop B, Ramachandran LK (1964) Progress in non-enzymatic selective modification and cleavage of proteins. Metabolism 13:1016–1025

Yola ML, Özaltın N (2011) Electrochemical studies on the interaction of an antibacterial drug nitrofurantoin with DNA. J Electroanal Chem 653:56–60

Zampakou M, Akrivou M, Andreadou EG, Raptopoulou CP, Psycharis V, Pantazaki AA, Psomas G (2013) Structure, antimicrobial activity, DNA- and albumin-binding of manganese(II) complexes with the quinolone antimicrobial agents oxolinic acid and enrofloxacin. J Inorg Biochem 121:88–99

Zhang Q, Liu J, Chao H, Xue G, Ji L (2001) DNA-binding and photo cleavage studies of cobalt(III) polypyridyl complexes: $[Co(phen)_2IP]^{3+}$ and $[Co(phen)_2PIP]^{3+}$. J Inorg Biochem 83:49–55